*Human Molecular Genetics, 2005, Vol. 14, No. 6* **859–871**
*doi:10.1093/hmg/ddi079*
*Advance Access published on February 9, 2005*

# A diastrophic dysplasia sulfate transporter (SLC26A2) mutant mouse: morphological and biochemical characterization of the resulting chondrodysplasia phenotype

**Antonella Forlino[1,‡], Rocco Piazza[1,‡], Cecilia Tiveron[2], Sara Della Torre[1], Laura Tatangelo[2,†], Luisa Bonafè[3], Benedetta Gualeni[1], Assunta Romano[1], Fabio Pecora[1], Andrea Superti-Furga[3], Giuseppe Cetta[1] and Antonio Rossi[1,*]**

[1]Dipartimento di Biochimica 'Alessandro Castellani', Università di Pavia, I-27100 Pavia, Italy, [2]Centro Ricerca Sperimentale, Istituto Regina Elena, I-00100 Roma, Italy and [3]Division of Molecular Pediatrics, Centre Hospitalier Universitaire Vaudois, 1011 Lausanne, Switzerland

Received August 3, 2004; Revised January 18, 2005; Accepted February 1, 2005 DDBJ/EMBL/GenBank accession no. D42049

**Mutations in the *diastrophic dysplasia sulfate transporter (DTDST* or *SLC26A2)* cause a family of recessively inherited chondrodysplasias including, in order of decreasing severity, achondrogenesis 1B, atelosteogenesis 2, diastrophic dysplasia (DTD) and recessive multiple epiphyseal dysplasia. The gene encodes a widely distributed sulfate/chloride antiporter of the cell membrane whose function is crucial for the uptake of inorganic sulfate, which is needed for proteoglycan sulfation. To provide new insights in the pathogenetic mechanisms leading to skeletal and connective tissue dysplasia and to obtain an *in vivo* model for therapeutic approaches to DTD, we generated a *Dtdst* knock-in mouse with a partial loss of function of the sulfate transporter. In addition, the intronic *neomycine* cassette in the mutant allele contributed to the hypomorphic phenotype by inducing abnormal splicing. Homozygous mutant mice were characterized by growth retardation, skeletal dysplasia and joint contractures, thereby recapitulating essential aspects of the DTD phenotype in man. The skeletal phenotype included reduced toluidine blue staining of cartilage, chondrocytes of irregular size, delay in the formation of the secondary ossification center and osteoporosis of long bones. Impaired sulfate uptake was demonstrated in chondrocytes, osteoblasts and fibroblasts. In spite of the generalized nature of the sulfate uptake defect, significant proteoglycan undersulfation was detected only in cartilage. Chondrocyte proliferation and apoptosis studies suggested that reduced proliferation and/or lack of terminal chondrocyte differentiation might contribute to reduced bone growth. The similarity with human DTD makes this mouse strain a useful model to explore pathogenetic and therapeutic aspects of DTDST-related disorders.**

## INTRODUCTION

Proteoglycans are a family of macromolecules characterized by one or more glycosaminoglycan (GAG) chains covalently linked to a core protein. They are present predominantly in the extracellular matrix or associated with the cell surface of eukaryotic cells, where they bind to other matrix and cell-associated components and to growth factors. Their specific functions derive from the chemical and structural diversity of either (or both) the polysaccharide or core protein part. The importance of proteoglycans as constituents of the extracellular matrix and of the cell surface is demonstrated by

*To whom correspondence should be addressed at: Dipartimento di Biochimica 'Alessandro Castellani', Via Taramelli, 3/B, I-27100 Pavia, Italy. Tel: +39 382987229; Fax: +39 382423108; Email: antrossi@unipv.it
†Present address: EMBL, Monterotondo, Rome, Italy.
‡The authors wish it to be known that, in their opinion, the first two authors should be regarded as joint First Authors.

differential expression during development and by disorders caused by mutations in genes encoding the core proteins or specific enzymes involved in their metabolism in human and animal models. GAGs are composed of characteristic repeating disaccharide units with sulfate groups at various positions and in different combinations. Sulfate groups attached to specific positions play important roles in the formation of biologically active domain structures and contribute to the high polyanionic charge of proteoglycans (1).

Sulfate groups are transferred from 3′-phosphoadenosine 5′-phosphosulfate (PAPS) to macromolecules by specific sulfotransferases. PAPS, the high-energy sulfate donor for macromolecular sulfation, is synthesized from cytoplasmic sulfate by PAPS synthase, a bifunctional enzyme with ATP-sulfurylase activity and adenosine 5′-phosphosulfate kinase activity (2). Intracellular sulfate comes either from the extracellular space or, to a lesser extent, from the intracellular catabolism of thiols (i.e. cysteine or methionine); the contribution of the two pathways to the intracellular sulfate pool depends on the cell type (3–7).

Owing to its anionic charge, extracellular sulfate is transported into the cytoplasm by specific anion transporters. The protein responsible for this transport appears to be the diastrophic dysplasia sulfate transporter (DTDST, also known as SLC26A2); the isolation of the gene coding for this sulfate/chloride antiporter of the cell membrane was the result of a long-term project aimed at elucidating the molecular basis of diastrophic dysplasia (DTD), a recessive skeletal dysplasia particularly frequent in the Finnish population (8), but present worldwide (9). Other sulfate transporters have been recently identified: SLC26A1, SLC26A3, SLC26A4 (previously known as SAT-1, CLD or DRA and PDS, respectively) and SLC26A5–A9 (10–17). Their expression is limited to specific tissues, suggesting that they play specific anion transport activities. On the contrary, DTDST is expressed in many tissues (8); however, the main phenotypic consequences of its functional impairment are restricted to bone and joints (18).

Mutations in the *DTDST* gene are associated with a family of recessively inherited chondrodysplasias including, in order of increasing severity, a recessive form of multiple epiphyseal dysplasia (rMED) (19), DTD (8), atelosteogenesis type 2 (20) and achondrogenesis 1B (21). Achondrogenesis 1B and atelosteogenesis type 2 are lethal before or shortly after birth; patients with DTD survive with major physical impairments, whereas the clinical phenotype in rMED is relatively mild (22). The mutations identified so far in DTDST chondrodysplasias include single amino acid substitutions or deletions, premature stop codons and reduced mRNA levels caused by splice-site mutations (9).

The main biochemical consequence of reduced intracellular sulfate levels caused by sulfate transport impairment is cartilage proteoglycan undersulfation. Thus, cartilage from DTDST patients has a reduced total sulfate content (21), contains undersulfated GAGs as shown by chondroitin sulfate disaccharide analysis and stains poorly with toluidine blue or alcian blue (23–25). On the basis of clinical, molecular and biochemical studies performed so far, a correlation has been traced between the different clinical phenotypes, the nature of the mutation in the DTDST, the residual activity of the sulfate transporter and cartilage proteoglycan undersulfation (23). Although DTDST is widely expressed, sulfation has not been measured in tissues other than cartilage. However, the presence of severe contractures in DTD patients suggests involvement of other connective tissues.

The importance of proteoglycan sulfation in skeletal development is also illustrated by a distinct, recessive form of spondyloepimetaphyseal dysplasia described in a large Pakistani family (SEMD Pakistani type) (26) and by its homologous murine model, the *brachymorphic* (*bm*) mouse (27); both conditions are caused by missense mutations in PAPS synthase 2 leading to a reduced function of the enzyme and thus reduced PAPS level. Cartilage proteoglycan undersulfation has been demonstrated in the animal model (28), whereas proteoglycan sulfation studies were not possible in SEMD Pakistani type patients.

The major involvement of cartilage in the human phenotypes of DTDST disorders, in SEMD Pakistani type and in the *bm* mouse demonstrates the crucial role of sulfate activation in the maturation of cartilage extracellular matrix macromolecules and the consequences of defects in this pathway on the architecture, composition and mechanical properties of cartilage as well as on the skeletogenesis. However, a detailed picture of the molecular and cellular events that could account for the specific defects in cartilage and bone matrix resulting in dwarfism, progressive joint disease and malformed skeleton is far from complete. To provide new insight on the role of proteoglycan sulfation in the development and homeostasis of the skeleton, we have generated the first mouse strain with a mutation in the *Dtdst* gene causing a partial loss of function of the sulfate transporter. We show that the mutation introduced in the murine *Dtdst* locus results in a skeletal and connective tissue phenotype, which reproduces at the clinical, morphological and biochemical level the human DTDST chondrodysplasias.

## RESULTS

### Generation of the Dtdst mutant mice

Transgenic mice harboring an A386V substitution in the eighth transmembrane domain of the DTDST were generated by homologous recombination in embryonic stem cells. To knock-in the A386V substitution, a C1184T transition was introduced by site-directed mutagenesis in a cloned fragment of exon 3. This mutation was detected in the homozygous state in a patient with a non-lethal form of DTD characterized by short stature, cleft palate, deformity of the external ear and ‘hitchhiker’ thumb deformity (9). A knock-out was considered unsuitable, because a total loss of function might result in lethality during the fetal period as observed in achondrogenesis 1B, the most severe condition in DTDST chondrodysplasias in humans.

A gene targeting vector was designed to knock-in the C>T transition in the murine *Dtdst* gene; for this purpose, the mouse *Dtdst* gene was isolated from a 129Sv/J mouse genomic bacterial artificial chromosome (BAC) library by polymerized chain reaction (PCR) screening using primers specific for exons 2 and 3. Both exons, which contain the whole coding sequence of the *Dtdst*, separated by an intron

of 1.8 kb as in the human homolog were identified in two clones. The genomic locus of the murine *Dtdst* was targeted with a replacement vector containing 8.3 kb of DNA sequence interrupted in intron 2 by the neomycin (neo) resistance cassette, driven by the phosphoglycerate kinase (PGK) promoter, for positive selection. For negative selection of non-homologous recombinants, the *herpes simplex thymidine kinase* was used, driven by the polyoma virus thymidine kinase (MC1) promoter (Fig. 1A). Embryonic stem clones that had undergone homologous recombination were identified by Southern blot analysis using two probes for the 5′ and 3′ end (Fig. 1B) of the targeted region. The 5′ end probe detected a 7.9 kb *BstX-I* fragment specific for the targeting allele and a 6.2 kb fragment for the wild-type allele; the 3′ end probe detected a 6.4 kb *Bsu36-I* fragment for the targeted allele and a 4.7 kb fragment for the wild-type allele. Two independent embryonic stem clones with an euploid karyotype were used to produce male chimeras; germline transmission of the targeted allele was achieved for both clones when bred to C57Bl/6J females. As expected, no apparent defects were observed in heterozygous animals. By mating heterozygous animals, homozygous mice were born in the expected Mendelian segregation ratio.

In the targeted allele, the *neo* gene was present in intron 2 at a *Hin*dIII site 174 bp upstream of the 3′ end of the intron, thus making the intron itself approximately twice as large as the wild-type. The consensus sequence for the branch site lies 22 nt upstream of the 3′ splice junction. To test whether the *neo* gene interfered with correct splicing, we studied the expression of the *Dtdst* by northern blotting of mRNA purified from skin (Fig. 1C). The expected 8 kb transcript was detected in the wild-type and, to a lesser extent, in hetero- and homozygous animals; both in hetero- and homozygous mutant animals, an additional band with a higher molecular weight was identified. This indicated that splicing of exon 2 onto exon 3 was impaired, most likely as a consequence of the *neo* gene within the intron. These data were confirmed by probing the northern blot with a *neo* probe, which hybridized only to the abnormal band (data not shown). The abnormal band was ∼40 and 60% of the total *Dtdst* transcript in hetero- and homozygous mutant animals, respectively. The total *Dtdst* transcript relative to *glyceraldehyde 3-phosphate dehydrogenase* was normal indicating that the presence of the *neo* gene do not interfere with mRNA degradation. Thus, in this mouse strain, functional impairment of the Dtdst was due not only to the knocked-in missense mutation, but also to a reduced level of correctly spliced transcript. In spite of the dual pathogenetic mechanism, the interesting phenotype of this first strain justified a detailed characterization.

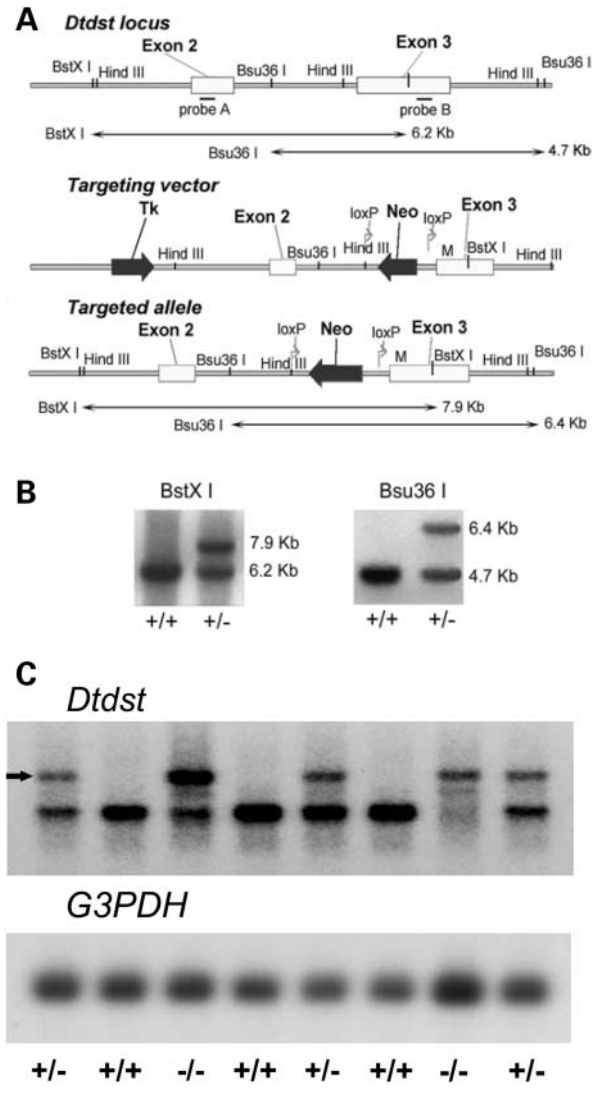


**Figure 1.** Gene targeting strategy of the *Dtdst* locus. (**A**) Schematic representation of the *Dtdst* locus, gene targeting vector and recombination at the *Dtdst* locus. The protein coding region of the Dtdst is distributed in exons 2 and 3. The gene targeting vector carrying the C>T transition (M) in exon 3 and a *neomycin (neo)* gene flanked by *loxP* sequences in intron 2 was electroporated in mouse embryonic stem cells. The targeted allele was obtained by homologous recombination between the gene targeting vector and a wild-type *Dtdst* allele. (**B**) Southern blot analysis of DNA from embryonic stem clones. The 7.9 kb *Bst*X I fragment and the 6.4 kb *Bsu*36 I fragment indicate proper 5′ and 3′ targeting of the *Dtdst* locus. The 6.2 kb *Bst*X I and 4.7 kb *Bsu*36 I fragments are from the wild-type allele. (**C**) Northern blot analysis of poly(A)$^+$ RNA from skin of pups at P1 hybridized with a *Dtdst* and a *glyceraldehyde 3-phosphate dehydrogenase* (*G3PDH*) probe. A band corresponding to the correctly spliced *Dtdst* transcript is detected in the wild-type (+/+), and, to a lesser extent, in heterozygous (+/−) and homozygous (−/−) animals. Both in hetero-and homozygous animals, an additional band (arrow) with a higher molecular weight is present indicating impaired splicing of exon 2 onto exon 3 caused by the *neo* gene within the intron.

### Phenotypic characterization of mutant mice

Mice heterozygous for the Dtdst mutation did not show any phenotypic changes, as is the case for carriers of DTDST mutations; body weight was normal, and no skeletal defects were observed by double staining with alcian blue and alizarin red of the skeleton (data not shown). All subsequent studies at the biochemical level failed to uncover any manifestation of heterozygosity: proteoglycan sulfation in cartilage, bone and skin were within normal values (data not shown), as well as sulfate uptake assay in chondrocytes (Fig. 6).

Homozygous animals were obtained by mating heterozygous mice. The phenotype of the offspring was observed from birth to 2 months of age by visual inspection; in addition,

skeletal development was studied by radiographic analysis and by double staining with alcian blue and alizarin red. At birth, mutant pups were alive and barely distinguishable from wild-type and heterozygous littermates: they were slightly shorter than wild-type littermates and the milk spot was smaller, indicating reduced viability (Fig. 2A). However, during the first days of life, mutant animals became easily identifiable because their growth was reduced; in addition, at postnatal day (P)14, thoracic kyphosis was observed at visual inspection. The kyphosis became progressively more pronounced until P60, when mutants had a characteristic posture with flexed head.

Body weight at birth was not significantly reduced when compared with wild-type mice, but delayed growth resulted in a reduction of ~60% at age P60 ($P < 0.0001$) (Fig. 3). Mortality of mutant animals was ~50% from birth to P21.

Overall motor activity of mutants was reduced, and adult animals had difficulties in climbing and hanging in the cage; for this reason, pelleted food had to be deposited directly onto the cage floor. Moreover, mutant animals sometimes walked backward rather than forward, a phenomenon that we interpreted as being related to pain or reduced mobility at the ischio-femoral and knee joints. In fact, in mice, the movement of hind leg joints are wider and potentially more painful when walking forward than backward.

Skeletal studies were performed from P1 to P21 by staining with alcian blue and alizarin red (Fig. 2B) and at P60 by X-rays (Fig. 2C). At birth, bending of the tibia was present, but no other skeletal abnormalities were observed. At P7, mutant mice developed thoracic kyphosis, which became progressively more severe at P14 and P21. In addition, mice showed bite overclosure (overgrowth of the mandible relative to the maxilla, resulting in lower incisors being placed anteriorly to upper incisors) and shortening of long bones. Ossification of skeletal elements was normal, on the basis of skeletal staining with alcian blue and alizarin red.

X-rays at P60 recapitulate the skeletal defects: shortening of tubular bones, severe thoracic kyphosis and abnormal thoracic cage with reduced volume, bite overclosure and hip dysplasia with pelvic deformity (Fig. 2C). Most homozygous mutant mice died before 6 months of age; on the basis of the clinical data, the direct cause of death could be the respiratory complications related to kyphosis, although we cannot exclude neurological problems or malnutrition due to dental malocclusion.

### Histological studies of epiphyseal cartilage

Sections of the tibial and femoral epiphysis from animals from P1 to P60 were stained with toluidine blue or with hematoxylin and eosin (H&E). In patients with DTDST disorders (with the exception of rMED), reduced staining of cartilage tissue sections with alcian blue or toluidine blue has been reported as a consequence of proteoglycan undersulfation. In mutant animals, cartilage matrix stained less intensely with toluidine blue when compared with age-matched wild-type littermates; in addition, some areas stained less than others with a patchy appearance (Fig. 4A). In mutant animals, chondrocyte size was more variable with many cells smaller than control ones.

We hypothesized that tubular bone shortening and reduced growth might be produced by changes at the growth plate, and we looked for this evidence in sections of the tibia. At P21, the overall architecture of the growth plate was preserved, with resting, proliferative and hypertrophic zones well defined. Columnization was present, and the width of the proliferative zone was not significantly different between mutant and wild-type animals on inspection. Chondrocyte apoptosis was evaluated in the growth plate by deoxynucleotidyltransferase-mediated dUTP-fluorescein nick end labeling (TUNEL) assay (Fig. 4B). In the wild-type, TUNEL-positive chondrocytes were present in the hypertrophic zone; whereas in mutant animals, cell death in the hypertrophic zone was reduced, suggesting that in mutant chondrocytes, there may be a delay in reaching the terminal differentiation that determines hypertrophy and death. A marked change in the growth plate was observed at P60: at low magnification, the growth plate appeared as a straight line in wild-type animals; whereas in mutant animals, it was irregularly delineated and in some regions appeared to be disrupted, with bony fusion of the epiphysis to the metaphysis (Fig. 5A and C). At higher magnification, few chondrocyte columns in the proliferative zone were evident (Fig. 5C). At the same age, we observed degeneration and fragmentation of articular cartilage of the knee joints and hypertrophy of the sinovia. In addition the long bones were osteoporotic: epiphyseal and metaphyseal trabecular structures were thinner, fewer and poorly connected to each other when compared with age-matched controls (Fig. 5C).

The formation of the secondary ossification center of the proximal epiphysis from the tibia was studied from P7 to P21 by H&E staining (Fig. 5B). In mice, the epiphyses are entirely cartilaginous at P1–P7; the formation of the secondary ossification center (P7–P14) initiates as a blood vessel penetrates from the articular surface into the epiphysis (P4) followed by differentiation of surrounding chondrocytes. In mutant animals, the penetration of the blood vessel from the articular surface seemed normal (data not shown). In the wild-type, the second ossification center was well developed at P14, whereas in mutant animals at the same age, its formation was still at the beginning, suggesting a delay in chondrocyte differentiation.

### Chondrocyte proliferation studies

To determine whether reduced bone growth in mutant animals was due to reduction in chondrocyte proliferation, we assessed the percentage of cells undergoing *de novo* DNA synthesis by 5-bromo-2-deoxy-uridine (BrdU) incorporation into primary chondrocyte cultures. For this purpose, cells were grown for 2 days, labeled with BrdU for the last 4 h of culture, and then stained with a specific anti-BrdU antibody. In mutant chondrocytes, the percentage of cells incorporating BrdU was significantly reduced compared with wild-type cells, suggesting a reduced proliferation capacity *in vitro* ($12 \pm 7$ and $20 \pm 8\%$, respectively; $P < 0.05$).

### Biochemical studies

The activity of the sulfate transporter was tested in fibroblasts and in primary cultures of chondrocytes and osteoblasts. Sulfate uptake assays were performed by pulse labeling

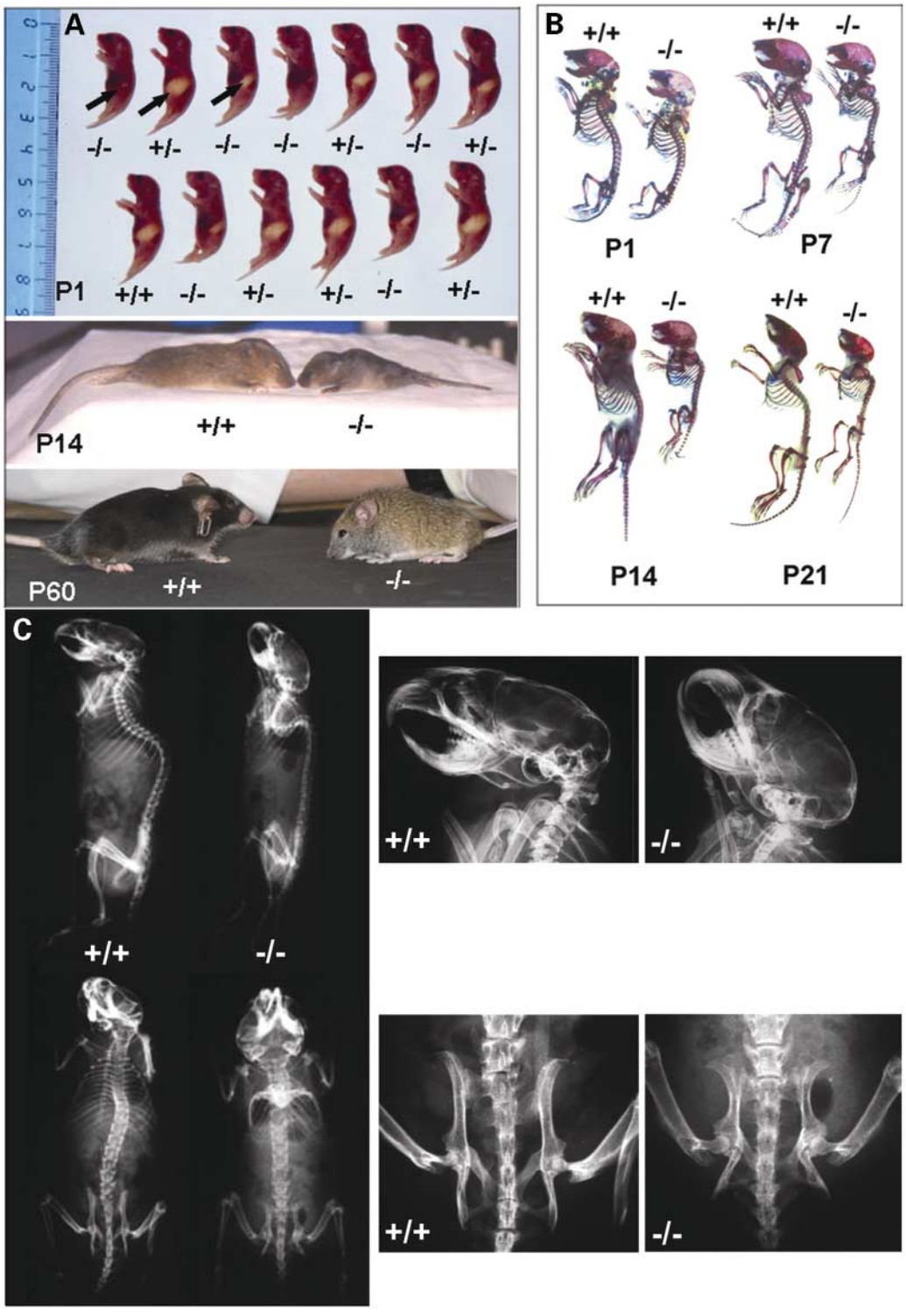


**Figure 2.** The morphologic features of homozygous animals for the *Dtdst* mutant allele are very reminiscent of human DTD. (**A**) The mutant (−/−) P1 pups are alive, slightly shorter than heterozygous (+/−) or wild-type (+/+) littermates. The milk spot (arrows) is smaller, indicating reduced viability when compared with heterozygous or wild-type animals. At visual inspection, a thoracic kyphosis is observed at P14 in mutant animals. Because of the kyphosis at P60, homozygotes show a characteristic posture with flexed head. (**B**) alcian blue (cartilage) and alizarin red (bone) staining of the whole skeleton. The thoracic kyphosis identified by visual inspection at P14 is already present at P7, causing deformity of the thoracic cage. In addition, mutant pups show bite overclosure and shortening of long bones. (**C**) X-rays at P60. In the mutant animal, shown at a higher magnification than the wild-type, shortening of tubular bones, severe thoracic kyphosis, bite overclosure and hip dysplasia are observed. The skull and the pelvis are shown at higher magnification to illustrate bite overclosure and hip dysplasia.

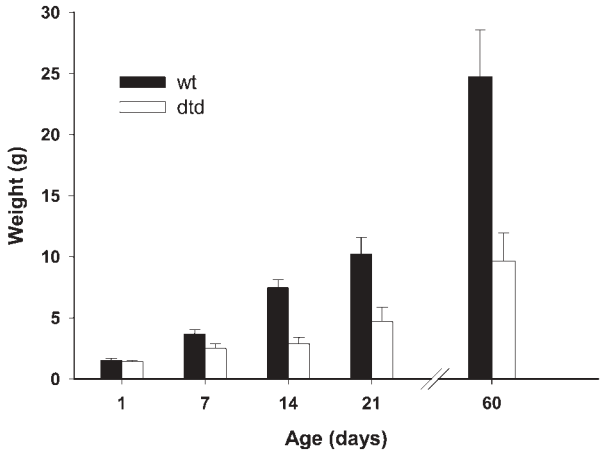


**Figure 3.** Body weight of mutant and wild-type mice from P1 to P60. The body weight confirms delayed growth of mutant animals resulting in a reduction of ~60% at P60. The average values with the standard deviation are shown for wild-type (wt) and mutant (dtd) animals ($n = 10–15$ for each age point; at P1, differences were not statistically significant; at the other age points $P < 0.05$).

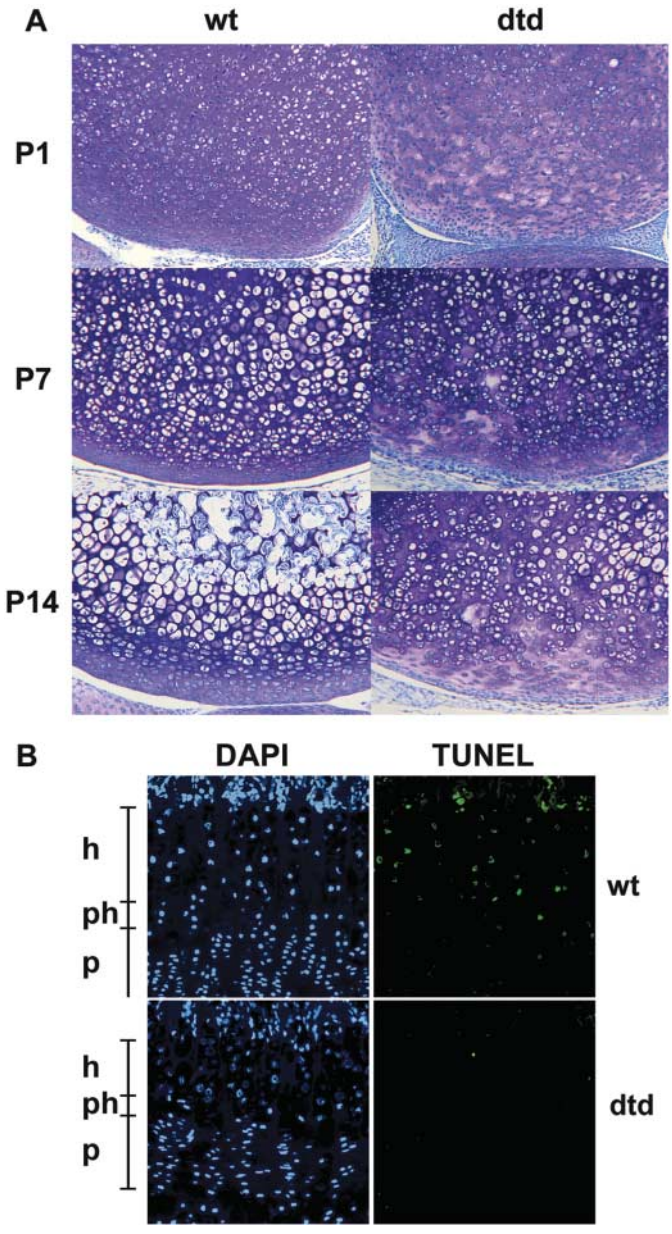


**Figure 4.** Decreased toluidine blue staining of cartilage from mutant animals and TUNEL staining of the growth plate. (**A**) In mutant animals (dtd), the cartilage matrix from the distal epiphysis of the femur is less intensely stained with toluidine blue when compared with wild-type (wt) animals with some areas staining less than other areas. In addition, chondrocytes are smaller and their size is more variable when compared with wild-type littermates. (**B**) Sections of the tibia of wild-type (wt) and mutant (dtd) animals at P21 were analyzed for the presence of apoptotic chondrocytes in the growth plate. In the wt apoptotic chondrocytes (green) were present in the hypertrophic region, whereas in the dtd, low frequency of apoptotic chondrocytes was detected in the whole growth plate. h: hypertrophic zone; ph, prehypertrophic zone; p, proliferating zone. Magnifications are 115× in (A) and 140× in (B).

with [$^{35}$S]sulfate for 1 min in medium containing varying concentrations of unlabeled sodium sulfate. In chondrocytes and fibroblasts from homozygous animals, the uptake was reduced at all sulfate concentrations tested when compared with wild-type or heterozygous animals (Fig. 6). These data validate our mouse model, because in patients with DTDST chondrodysplasias, sulfate uptake impairment has been observed in both cell types. Although it is known that the sulfate transporter is expressed in osteoblasts (29), sulfate uptake has never been studied in this cell type from patients with DTDST disorders. The same assay performed in osteoblasts from mutant animals showed sulfate uptake impairment suggesting that also in this cell type a large proportion of the intracellular sulfate pool is probably mediated by Dtdst (Fig. 6).

Sulfation of proteoglycans was then studied in different tissues of the mouse strain. It has been demonstrated (with the exception of rMED) that cartilage chondroitin sulfate proteoglycans are undersulfated in DTDST chondrodysplasias; however, even if tissue abnormalities are restricted to cartilage, no information is available regarding proteoglycan sulfation in other tissues such as skin or bone where the DTDST is expressed. For this reason, we measured proteoglycan sulfation in cartilage, skin and bone from mutant and wild-type animals. In addition, sulfation was measured at different ages from P1 to P60 to trace the course of proteoglycan sulfation during post-embryonic development in wild-type and mutant animals. Tissues were digested with papain to remove proteins and proteoglycan core proteins; GAGs were then recovered by cetylpyridinium chloride precipitation. After hyaluronic acid removal, chondroitin sulfate GAGs were digested with chondroitinase ABC and ACII, and released disaccharides were quantitated by HPLC. The degree of proteoglycan sulfation was measured as the amount of non-sulfated disaccharide (ΔDi-0S) relative to ΔDi-0S and mono-sulfated disaccharides (ΔDi-4S and ΔDi-6S). HPLC separation of cartilage samples demonstrated that in mutant animals, the relative amount of non-sulfated disaccharide was higher when compared with wild-types, providing direct evidence of reduced chondroitin sulfate proteoglycan sulfation (Fig. 7). Interestingly, in mutant animals, the highest values of proteoglycan undersulfation were

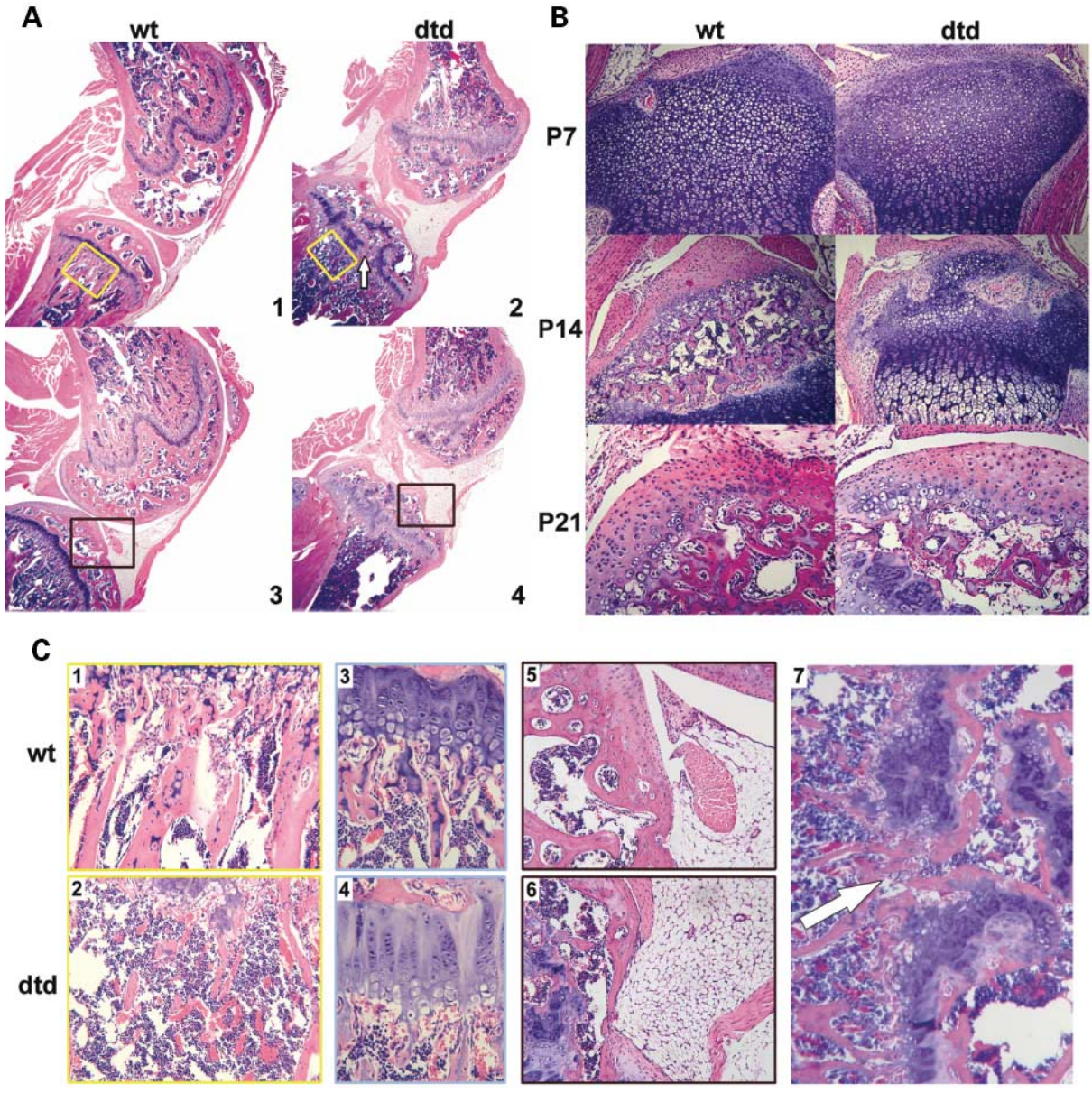


**Figure 5.** Structural alteration of the growth plate and delayed formation of the secondary ossification center. (**A**) H&E staining of the knees of animals, at P60. In mutant animals, the growth plate is irregularly delineated, and in some regions, it is disrupted with bony fusion of the epiphysis to the metaphysis (see arrow in A2 and magnification in C7). The areas enclosed in the boxes are shown at higher magnification in C1–2 and C5–6. (**B**) Formation of the secondary ossification center of the proximal epiphysis from the tibia from P7 to P21 in wild-type (wt) and mutant animals (dtd). At P14, the secondary ossification center is well developed in wt animals, but in the dtd, its formation is delayed suggesting a defect in chondrocyte differentiation. Sections are stained with H&E. (**C**) Enlarged views of bone tissue (panels 1 and 2), growth plate (panels 3 and 4) and articular cartilage (panels 5 and 6) at P60. In bone tissue, trabecular structures are thinner and poorly connected to each other when compared with age-matched controls (panels 1 and 2). Although less intense staining of matrix is evident, the sections of the tibial growth plate do not show significant differences in growth plate architecture, except for a possible rarefaction of chondrocytes and few chondrocyte columns in mutant animals (panels 3 and 4). Articular cartilage in mutant animals is degenerated and fragmented with sinovia hypertrophy (panels 5 and 6). Magnifications are 10× in (A), 70× in (B), 85× in C1–2, 125× in C3–4, 65× in C5–6 and 60× in C7.

observed at birth (∼32% of non-sulfated disaccharide versus 9.5% in controls, $P < 0.0001$), whereas proteoglycan sulfation increased with age, even if not within normal values. Proteoglycans obtained from the femoral diaphysis of mutant animals were slightly undersulfated and, as already observed in cartilage, sulfation increased with age (Fig. 7); unfortunately, we have no data concerning bone proteoglycan sulfation in mutant animals at P1 because of too small amount of bone available for the analysis.

Chondroitin/dermatan sulfate disaccharide analysis of skin from mutant animals showed that proteoglycan sulfation was comparable to that of wild-type animals at all age points considered (P1–P60) (Fig. 7), consistent with the lack of any phenotypic alteration of skin in the mouse strain, as well as in DTD patients.

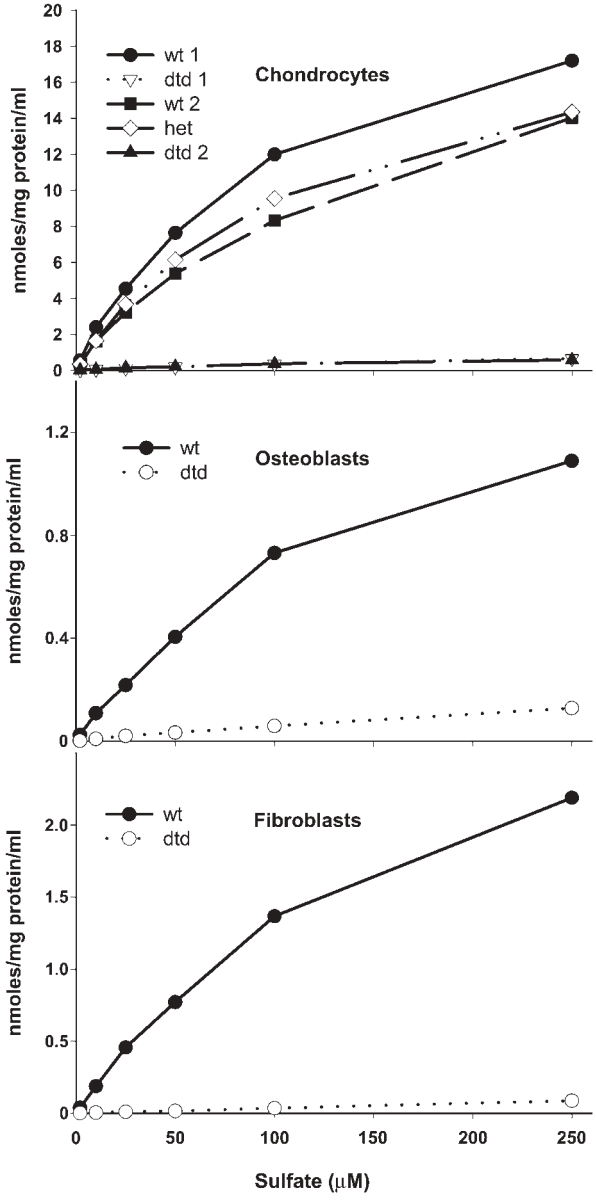


**Figure 6.** Functional assay of the Dtdst in different cell lines. Chondrocytes and osteoblasts in primary culture and skin fibroblasts from wild-type (wt) and mutant animals (dtd) were analyzed for uptake of inorganic sulfate. In the three cell lines considered, sulfate uptake is impaired in dtd animals, demonstrating that the chondrodysplasia phenotype is caused by targeting of the *Dtdst.* The activity of the sulfate transporter in the heterozygote (het) is within normal values confirming the lack of any phenotypic change in these animals. Sulfate uptake in chondrocytes was performed in two different wild-type mice, as well as in two dtd.

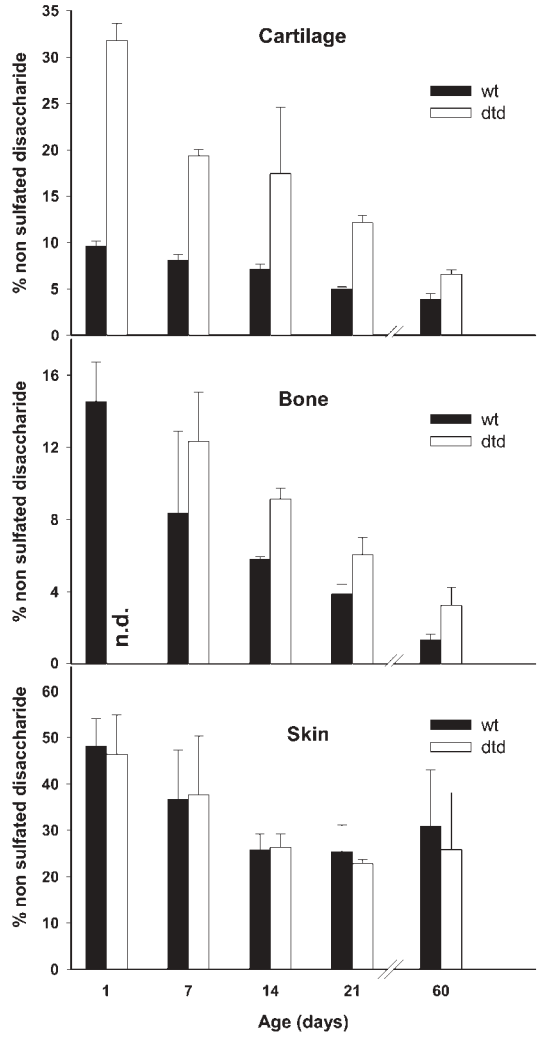


**Figure 7.** Sulfation of chondroitin sulfate proteoglycans in cartilage, bone and skin of animals at different ages from P1 to P60. The degree of proteoglycan sulfation has been determined by HPLC, on the basis of the amount of non-sulfated disaccharide (ΔDi-0S) relative to ΔDi-0S and mono-sulfated disaccharide (ΔDi-4S and ΔDi-6S). Analysis of cartilage from the femoral head demonstrates that in mutant animals (dtd), the relative amount of non-sulfated disaccharide is higher when compared with wild-type (wt) littermates, providing direct evidence of reduced chondroitin sulfate proteoglycan sulfation ($P < 0.05$). Interestingly, in mutant animals, the highest values of proteoglycan undersulfation are observed at birth, while sulfation increases with age. Proteoglycans obtained from the femoral diaphysis of mutant animals are slightly undersulfated and, as already observed in cartilage, there is an increase in sulfation with age ($P < 0.05$ at P7 and P14; at the other age point, differences were not statistically significant). Bone sulfation analysis in mutant animals at age P1 has not been possible, because of the reduced amount of bone available (n.d., not determined). Sulfation of skin proteoglycans in mutant animals is within normal values at all age points considered. Bars represent the average values with the standard deviation ($n = 4$) for wild-type and mutant animals.

## DISCUSSION

We have set out to generate a mouse model for skeletal dysplasias caused by mutations in the *Dtdst* gene. The strategy we designed consisted of knock-in of a single amino acid substitution that resulted in DTD of moderate severity in a human patient. The choice of a mutation associated with moderate severity in humans had been dictated by the aim of producing an affected but viable mouse and by the chance of generating a lethal phenotype during the perinatal period with a more severe mutation. The first strain of mice we obtained showed a phenotype that closely reproduced DTD, being characterized by dwarfism, skeletal deformities and joint contractures. Subsequent biochemical, histologic and radiographic analyses confirmed functional inactivation of Dtdst, thus

validating the model. RNA studies indicated that the *neomycin* gene in intron 2 interfered with splicing of the allele carrying the point mutation. Therefore, the pathogenesis of the chondrodysplasia phenotype in this strain comprises both the structural amino acid change and reduced levels of correct-sized, albeit mutation carrying, Dtdst mRNA caused by the splicing impairment. In spite of this observation, the model was not rejected because (i) most individuals affected by one of the DTDST dysplasias are not homozygote, but rather compound heterozygote for two of the many different known mutations, and compound heterozygosity for a null allele and a structural allele is frequent; (ii) all functional studies, in particular the sulfate uptake assay, confirmed the central role of sulfate transport inactivation in the pathogenesis of the observed phenotypic changes. In addition, as the observed phenotype was severe (50% mortality during the first 3 weeks), this mouse strain could provide new data concerning the role of proteoglycan sulfation during post-natal development of the skeleton. Thus, we proceeded with an in-depth characterization of the homozygous mutant mice during post-natal development from birth to P60.

Considering the species differences between humans and mice, the morphologic features of human DTD are well represented in the mutant mouse strain; in mutant animals, we observed reduced growth, craniofacial abnormalities, kyphosis and hip dysplasia. Phenotypic changes in mutant mice appear very early: at birth, the whole skeleton is smaller than that in wild-type littermates, and mutant pups show cartilage proteoglycan undersulfation and histological changes. Thus, the phenotype originates in the fetal period, demonstrating that the DTDST is functionally important in fetal development. Indeed, human DTDST chondrodysplasias (with the exception of the milder variant, rMED) can be diagnosed by ultrasound in the fetal period (30).

Histological studies of cartilage tissue sections also demonstrated similarities to human DTDST chondrodysplasia patients. Cartilage stained less with toluidine blue, a cationic dye with affinity to the sulfated, polyanionic proteoglycans. H&E and toluidine staining showed normal growth plate architecture at birth and during the first 3 weeks of age, but disorganization of the growth plate was marked at P60, explaining the postnatal component of growth failure. TUNEL assay on the tibial growth plate at P21 showed few apoptotic chondrocytes in the hypertrophic zone of mutant animals when compared with the wild-types. Chondrocyte apoptosis in endochondral ossification is a normal event linked to the progression of chondrocytes towards a terminally differentiated stage characterized by cell death and the formation of lacunae, followed by vascular invasion and bone formation (31). Reduced cell death in the hypertrophic zone of mutant animals might be linked to a delay in the differentiation process of chondrocytes. These data, together with the finding of reduced chondrocyte proliferation *in vitro*, suggest that reduced bone growth in DTDST disorders might be due to reduced chondrocyte proliferation and/or incomplete differentiation.

The finding of a delayed formation of the secondary ossification center is at discrepancy with the notion of accelerated bone maturation in human DTD patient; it is true though that definitive fusion of the epiphysis to the metaphysis approached in an early stage (P60) in the mutant mouse. Alkaline phosphatase staining of osteoblasts in primary culture from mutant mice was normal (data not shown) excluding a severe osteoblastic functional defect. Even if subtle osteoblast/osteoclast defects cannot be excluded, the osteopenic phenotype might be an indirect effect of abnormal cartilage matrix rather than an osteoblast defect. The issue of bone maturation thus remains to be determined with growth kinetic studies of epiphyseal growth cartilage.

We did not observe changes in the external ears similar to cystic swelling observed in DTD newborns, but this may be due to the fact that mouse ears are formed by soft fibrous tissue rather than by cartilage.

In cartilage of DTDST patients, the main biochemical consequence of reduced intracellular sulfate availability is proteoglycan undersulfation (23). For this reason, we measured cartilage proteoglycan sulfation in the femoral head cartilage of mutant mice. Chondroitin sulfate proteoglycans were undersulfated when compared with wild-type littermates (as is observed in human DTD), but interestingly, there was a progressive increase in proteoglycan sulfation with age (P1–P60). In DTDST disorders, the restriction of tissue alterations to cartilage has been linked to the high amount of proteoglycans synthesized by chondrocytes and thus to the ensuing high sulfate requirements. Previous studies performed in fibroblasts from DTDST patients demonstrated that the degree of proteoglycan sulfation depends also on the rate of proteoglycan synthesis: proteoglycan undersulfation was dramatically high when GAGs synthesis was enhanced by β-xylosides (23). As the intracellular sulfate pool is limited due to a reduced sulfate uptake per time unit, its depletion depends on proteoglycan synthesis rate and on proteoglycan species. Thus, the tendency to more normal proteoglycan sulfation observed in mutant mice over time may be explained by slower rate of proteoglycan synthesis in older mice. An additional factor that may affect proteoglycan sulfation comes from the formation of the secondary ossification center, which can provide sulfate and other sulfur compounds through the blood vessels penetrating the epiphyses and through the degradation of cartilage matrix with lysosomal catabolism of GAG chains (32,33).

A third factor modulating proteoglycan sulfation is intracellular sulfate recruitment from the oxidation of thiols (e.g. cysteine and methionine), which is significant in fibroblasts and chondrocytes from DTDST patients (24,34). We do not know to which extent this pathway is active *in vivo*, but the presence of blood vessels in the second ossification center may allow for sulfate recruitment from thiols.

The lack of any phenotype in skin (normal proteoglycan sulfation) is in agreement with the amount and type of proteoglycans present in this tissue when compared with cartilage. The amount of proteoglycans synthesized in skin is lower compared with cartilage, and in addition, versican and the small proteoglycans decorin and biglycan present in skin bears considerably less GAG chains compared with cartilage macromolecules (35). Thus, in fibroblasts, the intracellular sulfate pool remains adequate to allow for sulfation of skin proteoglycans.

Although the improvement in cartilage proteoglycan sulfation with aging, the histological and clinical data demonstrate

that the development of skeletal abnormalities is progressive, suggesting that other factors or sulfation of other macromolecules are involved in the pathogenesis of DTDST disorders. One possible explanation is that degenerative changes in cartilage are cumulative, and a late, partial recovery in proteoglycan sulfation may not be enough to restore tissue trophism. Another possible pathogenic mechanism for the progression of skeletal changes may involve heparan sulfate proteoglycans; these macromolecules are relevant for efficient FGFs signaling, which is crucial for the regulation of chondrocyte proliferation and differentiation (36). Moreover, they affect expression of other growth factors (i.e. Ihh) involved in endochondral bone formation (37). Several lines of evidence demonstrate that sulfation at specific positions along the GAG chains play crucial roles in the formation of biologically active domain structures independently from the overall level of sulfation (38). Sulfation of heparan sulfate proteoglycans has never been studied in DTDST disorders; however, it is likely that modulating the overall sulfation status and/or the sulfation at specific positions along the GAG chains will influence the availability of critical ligands and the optimal presentation of signaling molecules to their receptors.

Keratan sulfate GAGs are an additional family of sulfated oligosaccharide, which have so far not been studied in DTDST chondrodysplasias. Lumican and keratocan, the main keratan sulfate proteoglycans in the cornea, bear long, highly sulfated keratan sulfate chains. Interestingly, in the other tissues, these proteins occur as poorly sulfated or non-sulfated glycoproteins (39). Thus, even if visual impairment is not a feature of DTDST dysplasias, biochemical and ultrastructural analyses of the cornea in mutant animals would be worth of analysis. This hypothesis is further supported by the observation that macular corneal dystrophy, an autosomal recessive disorder with progressive punctate opacities in the cornea, is caused by mutations in the *N-acetylglucosamine-6-sulphotransferase* (*CHST6*) gene (40) leading to cornea keratan sulfate undersulfation (41).

To gain new insight into the function and properties of proteoglycans, several mouse strains have been generated in which specific sulfotransferases have been knocked-out (38). The mouse strain we have generated, together with the *bm* mouse, are the only ones with a defect in the sulfation pathway causing generalized undersulfation. Interestingly, although the biochemical consequences of the defect are the same (i.e. proteoglycan undersulfation), the two mouse strains show several differences. The *bm* phenotype is caused by a G79R substitution in PAPS synthase 2, which activates sulfate to PAPS, the universal sulfate donor for macromolecular sulfation; the mutation causes a partial loss of function of the enzyme leading to reduced PAPS level (27). *Bm* mice are normal in size at birth and the differences become apparent during the first 4 weeks of life, suggesting that the PAPS synthase 2 mutation specifically affects postnatal skeletal development and other PAPS synthases may be active and/or substitute PAPS synthase 2 during fetal development (27). In *bm* mice at P25, proteoglycans from rib cartilage were more undersulfated (>50% non-sulfated disaccaride) (28) than in our dtd mice. Taking into account the severity of proteoglycan undersulfation observed in cartilage from patients with DTDST disorders (23) and from the dtd mice, the *bm* phenotype should be more severe than observed. This suggests that other factors besides macromolecular sulfation affect the development and maintenance of the skeletal elements. Thus, it can be predicted that the identification of additional components of the sulfation pathway, of the proteoglycan metabolism and of the signaling pathways involved in the expression of extracellular matrix proteins, cytokines, growth factors and receptors in these animal models will provide new insight in protein sulfation and identify new pathogenetic mechanisms in inherited and/or acquired skeletal diseases.

In this study, we have generated a mouse strain with a partial loss of function of the Dtdst causing a non-lethal chondrodysplasia phenotype; the biochemical, histological and morphological studies validate this strain as a useful animal model of DTD to explore pathogenetic and therapeutic aspects of DTDST disorders. The non-lethal phenotype allows to study the influence of proteoglycan undersulfation on skeleton growth and maintenance, and therefore to trace the progression of the DTD phenotype. In addition, tissue-specific expression and sulfation of proteoglycans suggest that other tissues, not accessible in humans, might be altered (e.g. the cornea). No pharmacological treatment of DTD has been available so far; the demonstration that cysteine-derived compounds can increase the intracellular sulfate pool in chondrocytes suggests that pharmacological treatments might be tried to increase proteoglycan sulfation in the patients (34). No data are available *in vivo* concerning the contribution of this alternative pathway of sulfate recruitment to the sulfate pool and the effective dose required to increase proteoglycan sulfation in cartilage. The answers might be provided by the animal model before treatment of DTD patients might be considered.

## MATERIALS AND METHODS

### Molecular cloning of the *Dtdst* gene and construction of the gene targeting vector

To obtain the *Dtdst* gene, a 129Sv/J mouse BAC library (Genome System Inc.) was screened by PCR using sense and antisense primers corresponding to exon 2 (5′-AAAGAGCAGCATGACCTCTC-3′ and 5′-TTCAGGTCATATTTTGGGAGC-3′) and to exon 3 (5′-TGGGCTTTGTCTCTGTCTACC-3′ and 5′-CGTGTAGCCATGTTTCTTGGC-3′). Primers were designed according to the cDNA sequence available at Genbank (Accession no. D42049). Two clones were identified and were used to determine a restriction map of the DTDST locus by Southern analysis using two probes for exons 2 and 3, respectively. *Hin*dIII was found to cut the gene into two fragments of 5.2 and 3.2 Kb suitable for the gene-targeting vector. For subcloning of the two fragments, BAC clones were digested with *Hin*dIII and restriction digests analyzed by agarose gel electrophoresis. The regions on the agarose gel corresponding to 5 and 3 kb were cut, and DNA fragments in the agarose slices were subcloned in pBluescript II (Stratagene). Clones were then screened to find the ones containing the 5.2 and 3.2 kb inserts of the *Dtdst* gene. Once identified, the clones were sequenced to exclude recombination errors during subcloning and the DNA sequence was compared

to the same region on BAC clones. The C>T transition causing the A386V substitution in the Dtdst was introduced in the clone with the 3.2 Kb fragment by site-directed mutagenesis (GeneEditor, Promega). The 5.2 Kb *Dtdst* fragment and, after site-directed mutagenesis, the 3.2 Kb insert were then cloned in the gene targeting vector which was constructed from a basic targeting vector containing the *thymidine kinase* and *neo* genes for negative selection and positive selection, respectively (pKO Scrambler NTKV, Stratagene). The original vector was modified flanking the *neo* gene by *loxP* sequences for possible excision of the *neo* cassette by Cre recombinase after homologous recombination.

### Generation of targeted embryonic stem cells and mice

Electroporation of the linearized targeting vector into AB1 ES cells (kindly provided by Dr Alan Bradley, Baylor College, Houston TX, USA) was followed by exposure to the neomycin analogue G418 and ganciclovir. Survived colonies were isolated and screened by Southern blot analysis for the recombinant allele. Correct 5′ targeting was checked by DNA digestion with *Bst*X I and membrane hybridization with a *Bam*H I fragment 614 bp long spanning 455 nucleotides upstream the first codon to nucleotide 402 of the Dtdst cDNA, whereas correct 3′ targeting by digestion with *Bsu*36 I and hybridization with a 273 bp PCR fragment spanning nucleotides 2195–2467. Numbering of nucleotides is according to the cDNA sequence available at Genbank (accession no. D42049). Targeted embryonic stem cells were injected in BDF1 × C57Bl/6J mouse blastocysts, according to standard procedures (42). The resulting chimeric male mice were mated with C57Bl/6J females to yield heterozygous animals. Tail DNA was tested for the presence of the targeted allele, using the same strategy described for embryonic stem cell screening.

### Northern blot analysis

Total RNA was extracted from skin of newborn animals with Tri-Reagent (Sigma), according to the manufacturer's protocol. Approximately 250 μg of total RNA were used for purification of mRNA using oligo(dT)-biotin and streptavidin magnetic beads (mRNA Isolation Kit, Roche). Four micrograms of poly(A)$^+$ RNAs were separated by gel electrophoresis in 1.2% formaldehyde–agarose denaturing gel and blotted onto a nylon membrane (Hybond-N$^+$, Amersham Biosciences). Hybridizations with ULTRAHyb (Ambion) or Rapid-hyb (Amersham Biosciences) were performed using a 273 bp PCR fragment spanning nucleotides 2195–2467 of the *Dtdst* or a *glyceraldehyde 3-phosphate deydrogenase* probe for the housekeeping gene; both probes were radiolabeled with [$^{32}$P]dCTP using Ready-to-Go DNA labeling beads (Amersham Biosciences).

### Skeletal preparations and histochemistry

Skeletal preparations of mice ranging from P1 to P21 were made with an alcian blue–alizarin red method (43). Briefly, pups were skinned, dehydrated in 96% ethanol, defatted in acetone and stained with alcian blue and alizarin red. Muscles were then removed with 1% KOH; preparations were then stored in glycerol.

For histochemical studies, the whole limbs of animals were fixed with 10% formaldehyde in phosphate buffer saline and processed for light microscopy, according to standard procedure. Five micrometer sections were stained with H&E or with toluidine blue. For detection of apoptotic cells by fluorescence microscopy in tibia growth plate sections, a TUNEL assay (DeadEnd Fluorometric TUNEL System, Promega) was used, according to the manufacturer's instructions. Nuclei were counterstained with 4′,6-diamidino-2-phenylindole (DAPI).

### Cell cultures and sulfate uptake assays

Chondrocyte and skin fibroblast cultures were established from pups at P1, whereas osteoblast cultures from pups at P60. Skin fibroblasts were cultured in Dulbecco's modified Eagle's medium (DMEM) with 10% fetal calf serum (FCS) and antibiotics at 37°C in 5% $CO_2$. Chondrocytes were released from epiphyseal cartilage by digestion with 1 mg/ml collagenase A (Roche) in DMEM at 37°C overnight. Dissociated cells were washed with DMEM containing 10% FCS and plated in the same medium. To recover osteoblasts, the femoral diaphyses after bone marrow flushing were finely minced and digested with 1 mg/ml collagenase A in 10 ml DMEM/Ham's F-12K (1:1) at 37°C for 2 h. Bone fragments were then washed with DMEM/Ham's F-12K (1:1), seeded in Petri dishes and incubated in DMEM/Ham's F-12K (1:1) supplemented with 25 μg/ml ascorbic acid and 10% FCS. The osteoblastic phenotype was demonstrated by alkaline phosphatase activity (44).

For chondrocyte proliferation assay, primary cultured cells were grown on Lab-Tek Chamber Slides (Nunc) for 2 days at 37°C in 5% $CO_2$ in DMEM supplemented with 10% inactivated FCS and labeled in the same medium with BrdU for 4 h. At the end of the labeling period, detection of labeled cells was performed, according to the manufacturer's suggestions using the 5-bromo-2-deoxyuridine labeling and detection kit I (Roche). Cells were counterstained with DAPI. Percentage of cells incorporating BrdU was determined by counting positives on a total of 300 random nuclei in three independent experiments.

For sulfate uptake assays, the same protocol was used for either chondrocytes or osteoblasts in primary culture and for skin fibroblasts at passage 4. Cells were seeded in 10 cm$^2$ Petri dishes ($3 \times 10^5$ cells per dish) and incubated in DMEM (DMEM/Ham's F-12K 1:1 for osteoblasts) containing 10% FCS for 24 h at 37°C. Sulfate uptake was performed as described previously using low ionic strength buffer (1 mM $MgCl_2$, 300 mM sucrose, 10 mM Tris–HEPES, pH 7.5) containing concentrations of $Na_2SO_4$ ranging from 2 to 250 μM. In preparation for the assay, cells were washed three times with pre-warmed sulfate-free low ionic strength buffer and pre-incubated for 2 min in the same buffer at 37°C. Cells were then incubated for 1 min at 37°C in low ionic strength buffer containing different concentrations of $Na_2SO_4$ and a constant concentration (0.1 μM, corresponding to 150 μCi/ml) of carrier-free $Na_2[^{35}S]O_4$ (PerkinElmer Life Sciences). Following incubation, the uptake medium was removed and

cells were washed four times with 1.5 ml of ice-cold medium containing 100 mM sucrose, 100 mM $NaNO_3$, 1 mM $MgCl_2$ and 10 mM Tris–HEPES, pH 7.5. Cells were then lysed in 2% SDS and assayed for radioactivity and protein content.

### Chondroitin sulfate disaccharide analysis

Disaccharide analysis was performed in skin, cartilage and bone. Skin was carefully excised and freed from subcutaneous fat. Cartilage was obtained from the femoral heads of pups at P1–P60 by careful dissection under the microscope. In pups at P1 and P7, femoral heads were cartilagineous, and in pups at P14 and P21, the secondary ossification center was removed with a tapered scalpel; whereas in pups at P60, the whole cartilage cup was removed from the bony part of the femoral head by forcing with a blade. Bone was obtained from the diaphysis of the femora after careful removal of the periosteum and of bone marrow by flushing with phosphate buffer saline.

To recover GAGs, tissue specimens were digested with 10 U of papain (Sigma) in 0.1 M sodium acetate, pH 5.6, 5 mM EDTA and 5 mM cysteine at 65°C for 48 h with further supplementation of the same amount of papain after 24 h. For decalcification of bone samples, the digestion buffer contained 100 mM EDTA. After papain inactivation at 100°C, released GAGs were recovered by precipitation with 1% cetylpyridinium chloride. The precipitate was washed three times with 10% potassium acetate in 96% ethanol and with 96% ethanol, respectively. The precipitate was dried and solubilized in hyaluronidase buffer (20 mM sodium acetate, pH 6.0, 75 mM NaCl). Hyaluronic acid was removed by digestion with 4 U of *Streptomyces* hyaluronidase (Seikagaku Corp.) at 60°C overnight followed by ultrafiltration with Ultrafree − 0.5 Centrifugal filter units (Millipore). Purified GAGs were digested with 30 mU of both chondroitinase ABC and ACII (Seikagaku Corp.) in 30 mM sodium acetate, 30 mM Tris–acetate, pH 7.35, at 37°C overnight. Undigested products were removed by precipitation with four volumes of ethanol and storage at −20°C overnight (25,45). Supernatants containing disaccharides were evaporated and solubilized in water. Disaccharides were fractionated with a Supelcosil LC-SAX1 (Supelco) HPLC column ($4.6 \times 250$ mm$^2$) using a gradient of 5–400 mM $KH_2PO_4$, pH 4.5, at room temperature, and the elution profile was measured at 232 nm (23).

### Statistical analysis

Two-way analysis of variance was used to determine differences among groups. Tukey's test was used for multiple comparison; differences in chondrocyte proliferation were evaluated using Student's *t*-test. A $P$-value $<0.05$ was considered statistically significant.

## ACKNOWLEDGEMENTS

We thank Angelo Gallanti for expert cell culturing, Professor Laura Pozzi for the use of AB1 ES cells and Professor Ruggero Tenni for critical reading of the manuscript. This work was supported by grants from the Telethon-Italy (grant no. D.083 to A.R. and grant no. B.055 to C.T.), Fondazione Cariplo (to G.C.), MIUR PRIN (grant no. 20022052257 to G.C. and grant no. 2003052778 to A.R.), Swiss National Foundation (SNF Project 3100A0-100485 'Molecular Basis of Human Skeletal Dysplasias' to A.S.F. and L.B.) and Consorzio Interuniversitario per le Biotecnologie 2003 (to G.C.).

## REFERENCES

1. Habuchi, O. (2000) Diversity and functions of glycosaminoglycan sulfotransferases. *Biochim. Biophys. Acta*, **1474**, 115–127.
2. Venkatachalam, K.V., Akita, H. and Strott, C.A. (1998) Molecular cloning, expression, and characterization of human bifunctional 3′-phosphoadenosine 5′-phosphosulfate synthase and its functional domains. *J. Biol. Chem.*, **273**, 19311–19320.
3. Esko, J.D., Elgavish, A., Prasthofer, T., Taylor, W.H. and Weinke, J.L. (1986) Sulfate transport-deficient mutants of Chinese hamster ovary cells. Sulfation of glycosaminoglycans dependent on cysteine. *J. Biol. Chem.*, **261**, 15725–15733.
4. Elgavish, A. and Meezan, E. (1991) Sulfation by human lung fibroblasts: SO4(2-) and sulfur- containing amino acids as sources for macromolecular sulfation. *Am. J. Physiol.*, **260**, L450–L456.
5. Keller, J.M. and Keller, K.M. (1987) Amino acid sulfur as a source of sulfate for sulfated proteoglycans produced by Swiss mouse 3T3 cells. *Biochim. Biophys. Acta*, **926**, 139–144.
6. Ito, K., Kimata, K., Sobue, M. and Suzuki, S. (1982) Altered proteoglycan synthesis by epiphyseal cartilages in culture at low SO4(2-) concentration. *J. Biol. Chem.*, **257**, 917–923.
7. Humphries, D.E., Silbert, C.K. and Silbert, J.E. (1988) Sulphation by cultured cells. Cysteine, cysteinesulphinic acid and sulphite as sources for proteoglycan sulphate. *Biochem. J.*, **252**, 305–308.
8. Hästbacka, J., de la, C.A., Mahtani, M.M., Clines, G., Reeve Daly, M.P., Daly, M., Hamilton, B.A., Kusumi, K., Trivedi, B., Weaver, A. *et al.* (1994) The diastrophic dysplasia gene encodes a novel sulfate transporter: positional cloning by fine-structure linkage disequilibrium mapping. *Cell*, **78**, 1073–1087.
9. Rossi, A. and Superti-Furga, A. (2001) Mutations in the diastrophic dysplasia sulfate transporter (DTDST) gene (SLC26A2): 22 novel mutations, mutation review, associated skeletal phenotypes, and diagnostic relevance. [Erratum (2001) *Hum. Mutat*, 18(1),82.] *Hum. Mutat.*, **17**, 159–171.
10. Bissig, M., Hagenbuch, B., Stieger, B., Koller, T. and Meier, P.J. (1994) Functional expression cloning of the canalicular sulfate transport system of rat hepatocytes. *J. Biol. Chem.*, **269**, 3017–3021.
11. Schweinfest, C.W., Henderson, K.W., Suster, S., Kondoh, N. and Papas, T.S. (1993) Identification of a colon mucosa gene that is down-regulated in colon adenomas and adenocarcinomas. *Proc. Natl Acad. Sci. USA*, **90**, 4166–4170.
12. Scott, D.A., Wang, R., Kreman, T.M., Sheffield, V.C. and Karnishki, L.P. (1999) The Pendred syndrome gene encodes a chloride–iodide transport protein. *Nat. Genet.*, **21**, 440–443.
13. Ludwig, J., Oliver, D., Frank, G., Klocker, N., Gummer, A.W. and Fakler, B. (2001) Reciprocal electromechanical properties of rat prestin: the motor molecule from rat outer hair cells. *Proc. Natl Acad. Sci. USA*, **98**, 4178–4183.
14. Zheng, J., Shen, W., He, D.Z., Long, K.B., Madison, L.D. and Dallos, P. (2000) Prestin is the motor protein of cochlear outer hair cells. *Nature*, **405**, 149–155.
15. Lohi, H., Kujala, M., Kerkela, E., Saarialho-Kere, U., Kestila, M. and Kere, J. (2000) Mapping of five new putative anion transporter genes in human and characterization of SLC26A**6**, a candidate gene for pancreatic anion exchanger. *Genomics*, **70**, 102–112.
16. Lohi, H., Kujala, M., Makela, S., Lehtonen, E., Kestila, M., Saarialho-Kere, U., Markovich, D. and Kere, J. (2002) Functional characterization of three novel tissue-specific anion exchangers SLC26A7, -A8, and -A9. *J. Biol. Chem.*, **277**, 14246–14254.
17. Waldegger, S., Moschen, I., Ramirez, A., Smith, R.J., Ayadi, H., Lang, F. and Kubisch, C. (2001) Cloning and characterization of SLC26A6, a novel member of the solute carrier 26 gene family. *Genomics*, **72**, 43–50.
18. Superti-Furga, A. (2002) Skeletal Dysplasias related to Defects in Sulfate Metabolism. In Steinmann, B. and Royce, P. (eds.), *Connective Tissue and Its Heritable Disorders.* Wiley-Liss, New York, NY, pp. 939–960.

19. Superti-Furga, A., Neumann, L., Riebel, T., Eich, G., Steinmann, B., Spranger, J. and Kunze, J. (1999) Recessively inherited multiple epiphyseal dysplasia with normal stature, club foot, and double layered patella caused by a DTDST mutation. *J. Med. Genet.*, **36**, 621–624.
20. Hästbacka, J., Superti-Furga, A., Wilcox, W.R., Rimoin, D.L., Cohn, D.H. and Lander, E.S. (1996) Atelosteogenesis type II is caused by mutations in the diastrophic dysplasia sulfate-transporter gene (DTDST): evidence for a phenotypic series involving three chondrodysplasias. *Am. J. Hum. Genet.*, **58**, 255–262.
21. Superti-Furga, A., Hästbacka, J., Wilcox, W.R., Cohn, D.H., van der Harten, H.J., Rossi, A., Blau, N., Rimoin, D.L., Steinmann, B., Lander, E.S. *et al.* (1996) Achondrogenesis type IB is caused by mutations in the diastrophic dysplasia sulphate transporter gene. *Nat. Genet.*, **12**, 100–102.
22. Ballhausen, D., Bonafe, L., Terhal, P., Unger, S.L., Bellus, G., Classen, M., Hamel, B.C., Spranger, J., Zabel, B., Cohn, D.H. *et al.* (2003) Recessive multiple epiphyseal dysplasia (rMED): phenotype delineation in eighteen homozygotes for DTDST mutation R279W. *J. Med. Genet.*, **40**, 65–71.
23. Rossi, A., Kaitila, I., Wilcox, W.R., Rimoin, D.L., Steinmann, B., Cetta, G. and Superti-Furga, A. (1998) Proteoglycan sulfation in cartilage and cell cultures from patients with sulfate transporter chondrodysplasias: relationship to clinical severity and indications on the role of intracellular sulfate production. *Matrix Biol.*, **17**, 361–369.
24. Rossi, A., Bonaventure, J., Delezoide, A.L., Superti-Furga, A. and Cetta, G. (1997) Undersulfation of cartilage proteoglycans *ex vivo* and increased contribution of amino acid sulfur to sulfation *in vitro* in McAlister dysplasia/atelosteogenesis type 2. *Eur. J. Biochem.*, **248**, 741–747.
25. Rossi, A., Bonaventure, J., Delezoide, A.L., Cetta, G. and Superti-Furga, A. (1996) Undersulfation of proteoglycans synthesized by chondrocytes from a patient with achondrogenesis type 1B homozygous for an L483P substitution in the diastrophic dysplasia sulfate transporter. *J. Biol. Chem.*, **271**, 18456–18464.
26. ul Haque, M.F., King, L.M., Krakow, D., Cantor, R.M., Rusiniak, M.E., Swank, R.T., Superti-Furga, A., Haque, S., Abbas, H., Ahmad, W. *et al.* (1998) Mutations in orthologous genes in human spondyloepimetaphyseal dysplasia and the brachymorphic mouse. *Nat. Genet.*, **20**, 157–162.
27. Kurima, K., Warman, M.L., Krishnan, S., Domowicz, M., Krueger, R.C., Jr, Deyrup, A. and Schwartz, N.B. (1998) A member of a family of sulfate-activating enzymes causes murine brachymorphism. [Erratum *Proc. Natl Acad. Sci. USA* (1998), 95(20), 12071.] *Proc. Natl Acad. Sci. USA*, **95**, 8681–8685.
28. Wikstrom, B., Engfeldt, B., Heinegard, D. and Hjerpe, A. (1985) Proteoglycans and glycosaminoglycans in cartilage from the brachymorphic (bm/bm) mouse. *Coll. Relat. Res.*, **5**, 193–204.
29. Kobayashi, T., Sugimoto, T., Saijoh, K., Fukase, M. and Chihara, K. (1997) Cloning of mouse diastrophic dysplasia sulfate transporter gene induced during osteoblast differentiation by bone morphogenetic protein-2. *Gene*, **198**, 341–349.
30. Jung, C., Sohn, C. and Sergi, C. (1998) Case report: prenatal diagnosis of diastrophic dysplasia by ultrasound at 21 weeks of gestation in a mother with massive obesity. *Prenat. Diagn.*, **18**, 378–383.
31. Gibson, G. (1998) Active role of chondrocyte apoptosis in endochondral ossification. *Microsc. Res. Tech.*, **43**, 191–204.
32. Harper, G.S., Rozaklis, T., Bielicki, J. and Hopwood, J.J. (1993) Lysosomal sulfate efflux following glycosaminoglycan degradation: measurements in enzyme-supplemented Maroteaux–Lamy syndrome fibroblasts and isolated lysosomes. *Glycoconj. J.*, **10**, 407–415.
33. Rome, L.H. and Hill, D.F. (1986) Lysosomal degradation of glycoproteins and glycosaminoglycans. Efflux and recycling of sulphate and *N*-acetylhexosamines. *Biochem. J.*, **235**, 707–713.
34. Rossi, A., Cetta, A., Piazza, R., Bonaventure, J., Steinmann, B. and Superti-Furga, A. (2003) *In vitro* proteoglycan sulfation derived from sulfhydryl compounds in sulfate transporter chondrodysplasias. *Pediatr. Pathol. Mol. Med.*, **22**, 311–321.
35. Carrino, D.A., Sorrell, J.M. and Caplan, A.I. (2000) Age-related changes in the proteoglycans of human skin. *Arch. Biochem. Biophys.*, **373**, 91–101.
36. Ornitz, D.M. and Marie, P.J. (2002) FGF signaling pathways in endochondral and intramembranous bone development and human genetic disease. *Genes Dev.*, **16**, 1446–1465.
37. Kronenberg, H.M. (2003) Developmental regulation of the growth plate. *Nature*, **423**, 332–336.
38. Muramatsu, T. (2000) Essential roles of carbohydrate signals in development, immune response and tissue functions, as revealed by gene targeting. *J. Biochem. (Tokyo)*, **127**, 171–176.
39. Corpuz, L.M., Funderburgh, J.L., Funderburgh, M.L., Bottomley, G.S., Prakash, S. and Conrad, G.W. (1996) Molecular cloning and tissue distribution of keratocan. Bovine corneal keratan sulfate proteoglycan 37A. *J. Biol. Chem.*, **271**, 9759–9763.
40. Akama, T.O., Nishida, K., Nakayama, J., Watanabe, H., Ozaki, K., Nakamura, T., Dota, A., Kawasaki, S., Inoue, Y., Maeda, N. *et al.* (2000) Macular corneal dystrophy type I and type II are caused by distinct mutations in a new sulphotransferase gene. *Nat. Genet.*, **26**, 237–241.
41. Plaas, A.H., West, L.A., Thonar, E.J., Karcioglu, Z.A., Smith, C.J., Klintworth, G.K. and Hascall, V.C. (2001) Altered fine structures of corneal and skeletal keratan sulfate and chondroitin/dermatan sulfate in macular corneal dystrophy. *J. Biol. Chem.*, **276**, 39788–39796.
42. Ramirez-Solis, R., Davis, A.C. and Bradley, A. (1993) Gene targeting in embryonic stem cells. *Methods Enzymol.*, **225**, 855–878.
43. Forlino, A., Porter, F.D., Lee, E.J., Westphal, H. and Marini, J.C. (1999) Use of Cre/lox recombination system to develop a non-lethal knock-in murine model of osteogenesis imperfecta with an a1(I) G349C substitution. *J. Biol. Chem.*, **274**, 37923–37931.
44. Robey, P.G. and Termine, J.D. (1985) Human bone cells *in vitro*. *Calcif. Tissue Int.*, **37**, 453–460.
45. Harper, G.S., Hascall, V.C., Yanagishita, M. and Gahl, W.A. (1987) Proteoglycan synthesis in normal and Lowe syndrome fibroblasts. *J. Biol. Chem.*, **262**, 5637–5643.